Formation of Pb/63Sn Solder Bumps Using a Solder Droplet Jetting Method

Ho-Young Son, Jae-Woong Nah, *Member, IEEE*, and Kyung-Wook Paik, *Member, IEEE*

***Abstract*—Formation processes of Pb/63Sn solder droplets using a solder droplet jetting have not been sufficiently reported. Solving problems such as satellite droplets and position errors are very important for a uniform bump size and reliable flip-chip solder bump formation process. First, this paper presents the optimization of jet conditions of Pb/63Sn solder droplets and the formation process of Pb/63Sn solder bumps using a solder droplet jetting method. Second, interfacial reactions and mechanical strength of jetted Pb/63Sn solder bumps and electroless Ni–P/Au UBM joints have been investigated. Interfacial reactions have been investigated after the second solder reflow and aging, and results were compared with those of solder bumps formed by a solder screen-printing method. Third, jetted solder bumps with variable bump sizes have been demonstrated by a multiple jetting method and the control of waveform induced to a jet nozzle. Multiple droplets jetting method can control various height and size of solder bumps. Finally, real applications of jetted Pb/63Sn solder bumps have been successfully demonstrated on conventional DRAM chips and integrated passive devices (IPDs).**

***Index Terms*—Multiple jetting, Pb/Sn jetting, solder droplet jetting.**

I. Introduction

RECENTLY, flip-chip interconnection draws much attention because of miniaturization and higher electrical performance than conventional wire bonding or tape automated bonding (TAB) [1]. Among various flip-chip technologies, solder flip-chip has been widely used. Solder bumps using electroplating and screen-printing methods have been commonly used. However, both electroplating and screen-printing methods have their own limitation in terms of cost and bump size. The electroplating technique is suitable for small bump size less than 150 μm in diameter, but has a higher processing cost. On the other hand, the screen-printing technique has advantages of easier processes and lower cost, but it has limitations for smaller size and finer pitch bump formation. The brief comparison among various solder bumping technologies is presented in Table I, [2]–[4].

Contrary to above conventional methods, the solder droplet jetting method is compatible in both cost effectiveness and smaller size bump formation. Solder bumps in this method are separately jetted and fabricated on target positions of a moving substrate. It has easier process steps and can achieve low cost resulting from high coverage of solder bumps and no extra equipments except for substrates to be jetted and molten solder [3], [5]. Additionally, since the size of solder bumps in this way is approximately equal to the orifice diameter of the jet nozzle, bump size, and pitch with several tens of micrometers are feasible.

TABLE I
BRIEF COMPARISON OF SOLDER BUMPING METHODS [2]–[4]

	Electroplating	Screen/Stencil printing	Solder jetting
Tool requirement	Mask	Stencil mask	None
Cost	Very high	Medium	Low
Equipment	Sputter, Mask aligner, Plating tool	Solder paste printer	Solder jetting machine
Throughput	High	Very high	Medium
Minimum bump size (μm)	25	100	50
Minimum pitch (μm)	50	200	60
3D packaging	No	No	Yes
Solder alloy flexibility	Low	Medium	High

In spite of these advantages of the solder droplet jetting method, the optimization of solder droplets has not been well organized, and the characterization of jetted solder bumps has not been clearly discussed [5]–[7]. Moreover, applications of this technique on real devices have not been reported. Therefore, one of two objectives of this study is to optimize jetting conditions of stable solder droplets. After Pb/63Sn solder bumps are fabricated on electroless Ni–P/Au under bump metallurgy (UBM), the investigation on their interfacial reactions and mechanical properties will be presented. Second, flip-chip assembly of low-pass filter integrated passive devices (IPDs) and DRAM chips using jetted solder bumps will be demonstrated.

II. Experiments

Fig. 1 shows the solder droplet jetting system used in this study. In this system, based on the principle of drop-on-demand of ink-jet printers, molten solder droplets are jetted at target positions on a moving substrate [5]. The solder jet system consists of the following parts: A pneumatic part with a nitrogen gas system pushing down molten Pb/63Sn solder; a thermal part of a heating system used for melting solder; and an electrical part applying wave signals to the jet nozzle. Jet heads and jet nozzles

Manuscript received November 29, 2003; revised February 14, 2005. This work was supported by the Center of Electronic Packaging Materials (CEPM), Korea Science and Engineering Foundation.

H.-Y. Son and K.-W. Paik are with the Korea Advanced Institute of Science and Technology (KAIST), Daejeon 305–701, Korea (e-mail: hyson@kaist.ac.kr).

J.-W. Nah is with the Department of Materials Science and Engineering, the University of California, Los Angeles, CA 90095-1595 USA.

Digital Object Identifier 10.1109/TEPM.2005.853068

(a)

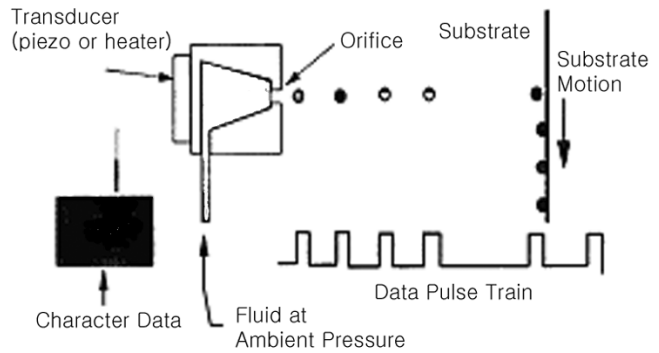

(b)

Fig. 1. (a) Solder droplet jetting system. (b) Schematic diagram of solder droplet jetting.

were supplied by MicroFab Inc., and the orifice diameter of the jet nozzles was 60 μm.

First of all, in order to optimize the jet conditions for a solder droplet formation, the effects of various jet variables such as the waveform induced to jet nozzle, jet height, overheating temperature, and substrate temperature, were divided by several different jet modes. The jet condition that had the minimum satellite droplets, one of the most important criterions for stable droplets, was determined for a certain bump size. To verify this in detail, after 48 solder droplets were jetted on chips with electroless Ni/Au UBM by changing voltage of wave signals and overheating temperature, the number of satellite droplets was measured by an optical microscope.

After this, 50- and 120-μm Pb/63Sn solder bumps were fabricated on electroless Ni–P/Au UBM using an optimized jet condition followed by solder droplet reflowing. Electroless Ni–P/Au UBM can be well combined with jetted solder bumps because it has a low processing cost and can be easily formed. Solder reflow was performed under a reflow profile with a flux activation region at 150 °C for 1 min and a peak region at 220 °C for 1 min. Liquid flux was spread on jetted solder bumps through a micropipette before solder reflowing. This process can be uniquely used in a solder jetting method because solder droplets had low adhesion with electroless Ni–P/Au UBM.

Next, to characterize the interfacial reactions between solder bumps and electroless Ni–P/Au UBM, jetted solder

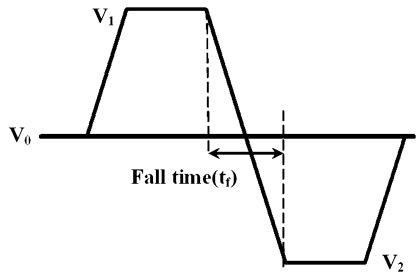

Fig. 2. Wave signal applied to a piezoelectric jet nozzle.

bumps were additionally reflowed for 1, 2, 4, 8, and 16 min at 220 °C and aged for 50, 100, 150, 250, and 500 h at 150 °C. Solder/UBM interfaces were observed by a scanning electron microscope (SEM) and were compared with those formed by a solder screen-printing method. Also, the shear strength of jetted solder bumps was measured by a bump shear test. Then, actual applications of the solder jetting technique on DRAM devices and low-pass filter IPDs were demonstrated. Their electrical resistance and high-frequency characterization were also measured.

Finally, solder bumps with various sizes were demonstrated after multiple jetting of one to ten droplets on Al/electroless Ni/Au UBM pads of 50, 85, and 120 μm in size.

III. Results and Discussion

A. Optimization of Solder Droplets Jetting Conditions

Fig. 2, shows the waveform of the electrical signal applied to a jet nozzle. When the voltage rose up to V_1 from base voltage (V_0) and then fell down to V_2, the piezoelectric device in the jet nozzle repeated the expansion and shrinking from original status. At that time, the molten solder flowed in the jet device was ejected out and jetted on substrates as a form of droplets [4], [5], [8]. When the wave signal was induced, the three voltage parameters (V_0, V_1, V_2), and fall time, time to need for falling down from V_1 to V_2, mainly affected the formation of stable solder droplets. The five different phenomena under unstable jetting conditions were presented in Fig. 3, [6], and [7]. Among them, satellite droplets and low position accuracy of droplets were the most important status to be considered, as shown in Fig. 4:

1) no jet;
2) big droplets or solder stream;
3) satellite droplets;
4) low position accuracy;
5) omission or excess of solder droplets.

1) Effects of Jet Variables on Solder Droplet Formation:

a) Nitrogen back pressure: For pushing down molten solder in the reservoir, nitrogen back pressure was applied. Several jet modes of solder droplets as a function of back pressures are shown in Table II. When the back pressure was less than 0.5 lbf/in^2, no droplets were ejected because the back pressure was not enough to push down the molten solder. Under 0.8 to 1.2 lbf/in^2, meta-stable conditions including some satellite droplets were observed. For higher back pressure, a jitter of solder droplets occurred, or big droplets and a solder stream

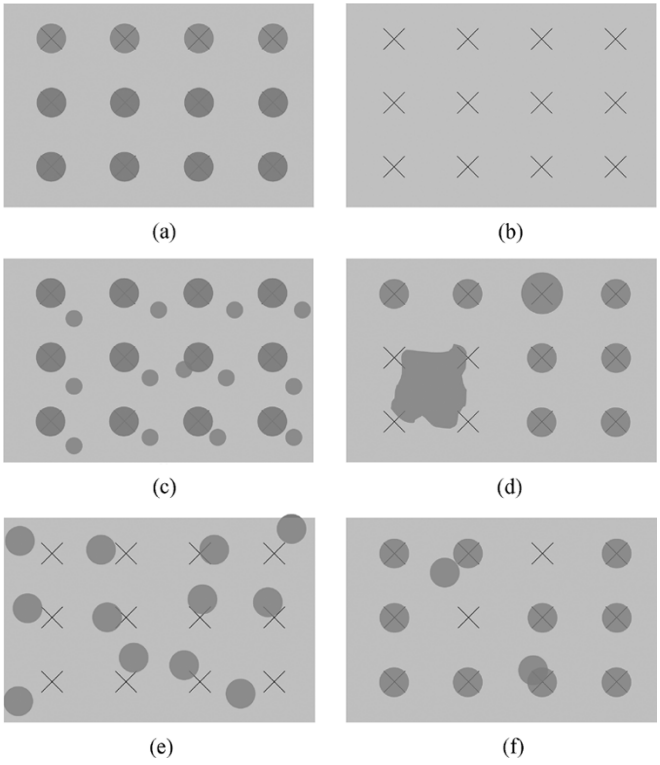

Fig. 3. Schematic diagram of several jet statuses. (a) Ideal case. (b) No jet. (c) Satellite droplets. (d) Big droplets or solder stream. (e) Low position accuracy. (f) Omission or excess of droplets. (X : target position, O : solder droplet).

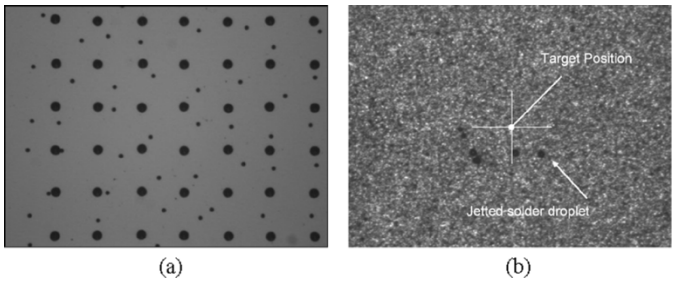

Fig. 4. (a) Satellite problems. (b) Position error of jetted solder droplets.

TABLE II
EFFECTS OF NITROGEN BACK PRESSURE ON JET STATUS

Back pressure (psi)	< 0.5	0.8~1.2	0.8~1.2	1.2~1.5	1.5~3.0	3.0~
Jet status	No jet	Satellites	Stable jet	Satellites	Big droplets or jitter	Solder stream

occasionally were generated from a jet nozzle [6]. Finally, after the approximate jet condition was determined as nitrogen back pressure of 0.8–1.2 lbf/in^2, a more detailed jetting condition was decided by determining the wave signal induced to a jet device.

Moreover, the nitrogen shroud flow that prevented molten solder around the orifice just after jetting was determined to be 1.5–3 sccm. The excess shroud flow caused a position error of a jetted solder droplet. Position error imported that any part of a jetted solder droplet did not spread over UBM pads of target position. Because the solder droplet was not wettable with UBM pads in this case, it cannot be self-aligned after solder reflow. The verification of position error was automatically performed by the jetting software. It was inspected through position scanning after solder jetting.

b) Waveform induced to a jet device: The electrical waveform induced to a jet nozzle was the most important factor in optimizing the jet conditions of solder droplets. Satellite droplets were distinctively generated according to base voltage (V_0), the maximum voltage (V_1), the minimum voltage (V_2), and the voltage difference ΔV. As shown in Fig. 5, the minimum satellite droplets were ejected under a specific voltage. Therefore, the selected voltages of the waveform were $V_0 = -100$ V, $V_1 = -64$ V, and $V_2 = -137$ V.

In addition, the size of the initial solder droplets varied according to a voltage difference ΔV. Fig. 6 shows the images of solder droplets jetted on a substrate at various voltage differences. At high ΔV, the contact area of a droplet with a substrate became larger. The biggest diameter changed from 69.3 μm for $\Delta V = 72$ V to 79.7 μm for $\Delta V = 88$ V. In general, the increase in ΔV led to the increase of drop speed of jetted droplets, but led to the formation of satellite droplets. At $\Delta V = 80$ V, solder droplets had the minimum satellite droplets. At any other ΔV values, satellite droplets did not reduced as the case of $\Delta V = 80$ V no matter how other voltage parameters were changed.

c) Temperature of molten Pb/63Sn solder in reservoir: The temperature of molten Pb/63Sn solder, the so-called overheating temperature, could also alter the number of satellite droplets. Fig. 7 presents the number of satellite droplets as a function of overheating temperature and base voltage of waveform, V_0. When molten solder was at 190 °C or 195 °C, many satellite droplets were generated regardless of V_0. However, when molten solder was at 200 °C, they were diminished to zero for $V_0 = -100$ V. Also, if the temperature was 210 °C, the number of satellite droplets became almost zero at broader ranges of V_0.

d) Jet height: Jet height, the distance from a jet nozzle to a substrate, mainly affected shapes and the position of jetted droplets as shown in Figs. 8 and 9. The increase of jet height led to the decrease of surface ripple, and then jetted solder droplets had smooth surfaces. The change of droplet shape resulted from the increase of the recoil of the droplet [7]. Fig. 9 shows the position accuracy of droplets as a function of jet height. Solder droplets should be jetted on electroless Ni UBM pads, because solder bumps can be self-aligned during solder reflow. However, in case solder droplets were jetted without touching the Ni pad during solder jetting, solder droplets were detached from Ni pads after reflow. When the jet height was more than 2.3 mm, position accuracy of jetted solder droplets rapidly decreased with jet heights. It was presumably because jetted solder droplets did not fall down vertically. In this study, preferred jet height was determined to be 1.0 mm.

e) Substrate temperature: Increase of substrate temperatures had no direct effects on stable droplet formation. However, since substrate temperature increased, solder droplets became near sphere shapes due to an increase of solidification time [7]. However, the shape of solder droplets might not be considered because they have no difference of shape after solder reflow. The delay of solidification might bring stronger adhesion

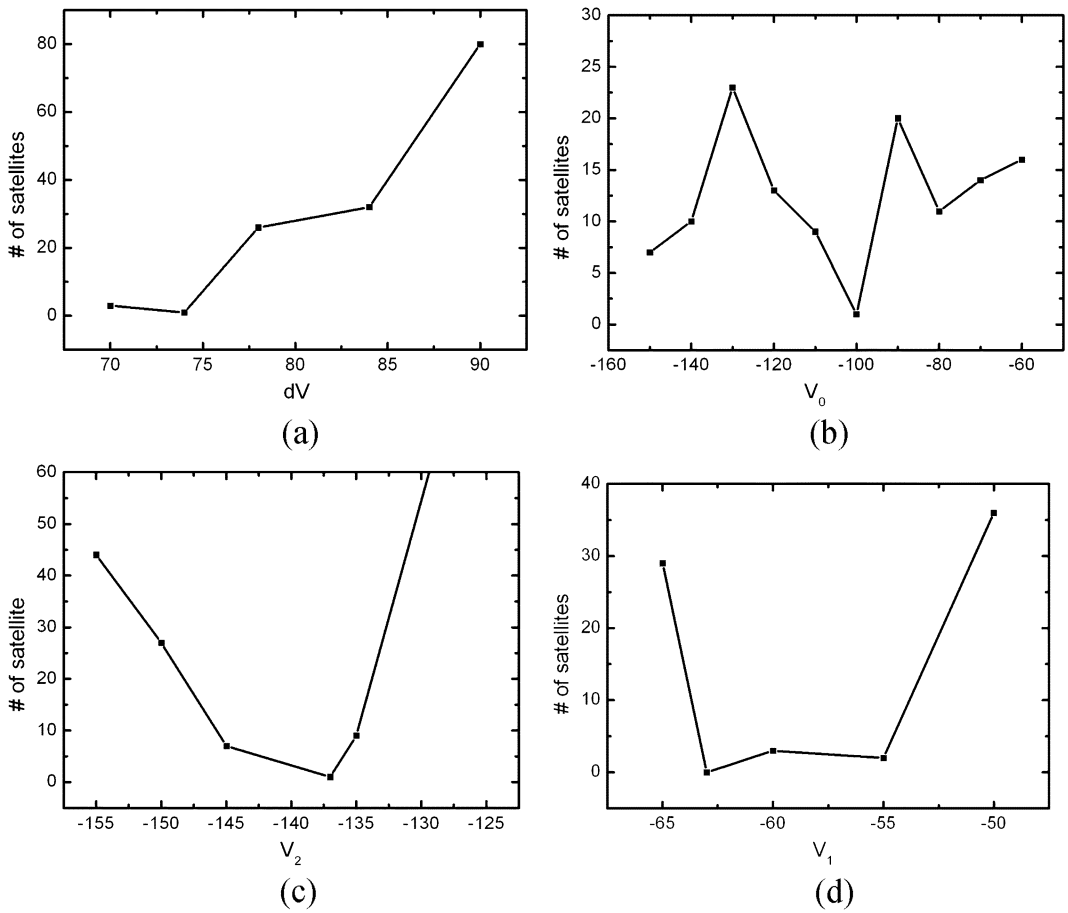

Fig. 5. Effects of waveform parameters on number of satellite droplets. (a) Voltage drop ΔV. (b) Base voltage V_0. (c) Minimum voltage V_2. (d) Maximum voltage V_1.

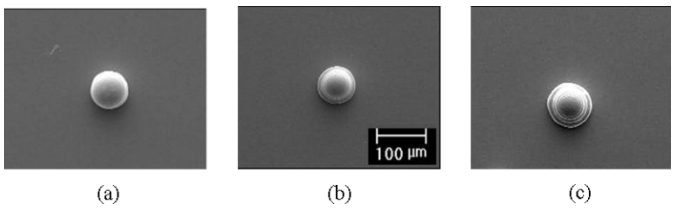

Fig. 6. Droplet shape changes as a function of ΔV.

of solder droplets because of more solder/UBM interfacial reactions. However, adhesion strengths of jetted solder droplets on Ni UBM at various substrate temperatures did not change at all, as shown in Table III. These results mean that solder droplets just after jetting did not sufficiently react with Ni UBM. The adhesion strength of solder droplets can be improved by the solder bump reflow process.

B. Fabrication and Characterization of Pb/63Sn Solder Bumps by Solder Jetting

Optimized jet conditions were finally determined, as shown in Table IV. Using these jet conditions, solder droplets were jetted on 5-μm-thick electroless Ni/Au UBM with pad size of 50 and 120 μm, and then solder bumps were fabricated by reflowing of solder droplets. Fig. 10 shows SEM images of solder bumps after reflow.

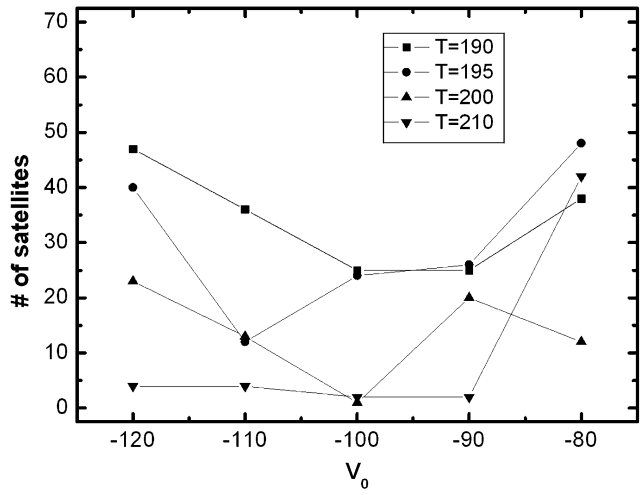

Fig. 7. Number of satellites versus V_0 graph as a function of overheating temperature.

Interfacial reactions between jetted solder/UBM were compared with those of screen-printed solder bumps, as shown in Fig. 13. Both cases show similar IMC growth rates and Ni UBM consumption rates. This result demonstrates that a solder droplet jetting method can be adopted as one of rework methods of omitted solder bumps formed by a screen-printing method. Next, the interfacial reactions between jetted Pb/63Sn solder

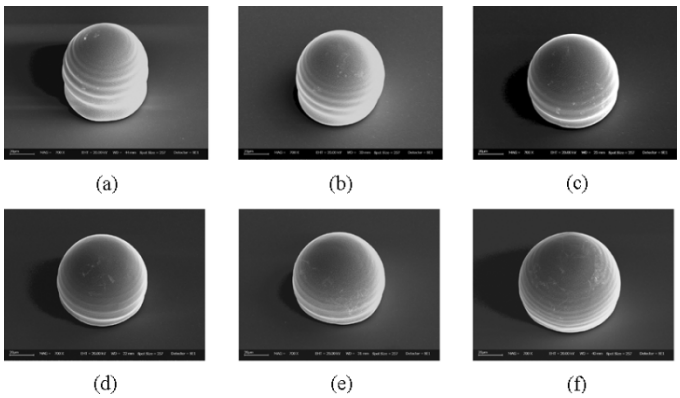

Fig. 8. Shapes of solder droplets at various jet heights. (a) 0.6 mm. (b) 1.0 mm. (c) 2.0 mm. (d) 2.9 mm. (e) 4.0 mm. (f) 5.0 mm.

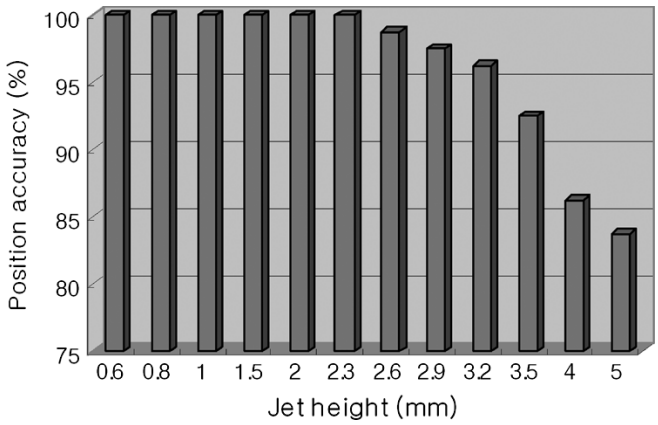

Fig. 9. Position accuracy versus jet height.

TABLE III
SHEAR STRENGTHS OF SOLDER DROPLETS JUST AFTER JETTING AT VARIOUS SUBSTRATE TEMPERATURES

Substrate temp. (°C)	Shear strength (gf)	Substrate temp. (°C)	Shear strength (gf)
30	9.0 ± 0.7	100	8.1 ± 1.4
60	4.6 ± 1.3	110	9.4 ± 1.4
90	5.4 ± 1.4	120	10.4 ± 1.4

TABLE IV
OPTIMIZED JET CONDITIONS OF SOLDER DROPLETS

Waveform parameters	Conditions	Variables	Conditions
Rise time	810μs	N_2 back pressure	0.8~ 1.2psi
Dwell time	2μs	N_2 shroud flow	2sccm
Fall time	43μs	Jet height	1mm
Echo time	2μs	Overheating temp.	200°C~210°C
F_rise time	810μs	Sub. Temp.	30°C
V_0	-100V		
V_1	-63V		
V_2	-137V		

bumps and electroless Ni UBM were investigated by SEM observation. Figs. 11 and 12 show SEM backscattered (BS) images of the solder/UBM interface and the thickness changes of the UBM layer and the intermetallic compound (IMC) layer after the second reflow. Sn atoms in Pb/63Sn solder bump reacted with Ni atoms, and Ni–Sn compounds were formed

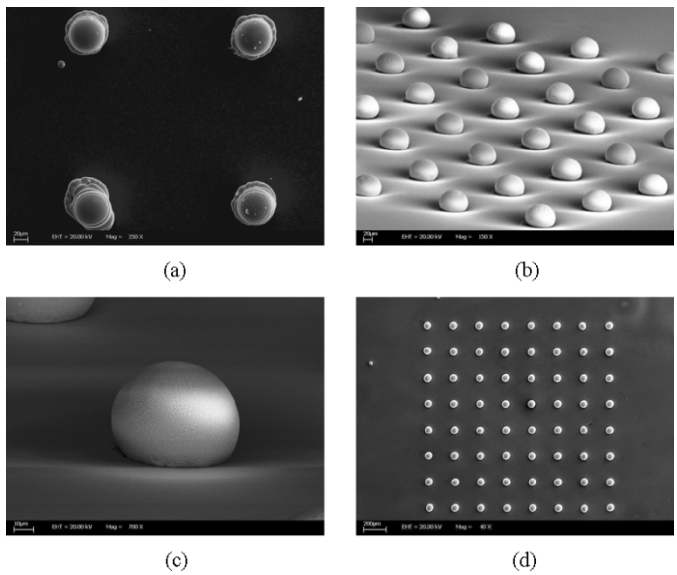

Fig. 10. SEM images of solder droplets and solder bumps. (a) Solder droplet just after jetting. (b) Reflowed solder bumps (×150). (c) Reflowed solder bump (×700). (d) Top view of arrayed jetted solder bumps (×40).

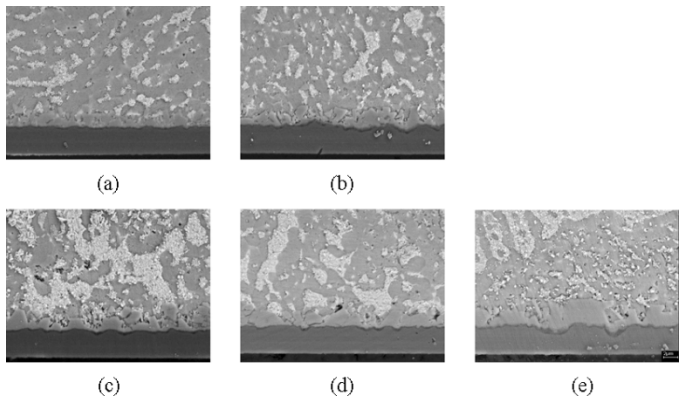

Fig. 11. SEM images of Pb/63Sn solder bumps and UBM interface with various reflow times at 220 °C (×3000). (a) 1 min. (b) 2 min. (c) 4 min. (d) 8 min. (e) 16 min.

between Ni UBM and solder bumps. As the second reflow times increased, the Ni–Sn IMC layer became thicker resulting in more Ni UBM consumption. The Ni–Sn compound formed at the solder/UBM interface was found to be Ni_3Sn_4 compounds by SEM-energy dispersive X-ray (EDX) analysis after solder etching.

Bump shear test results shown in Fig. 14 show that adhesion strength of solder bumps can be improved by reflow; however, bump shear strength slightly decreases with longer heat treatment times. These shear results of jetted solder bumps had no significant differences with that of screen-printed solder bumps.

C. Various Solder Bump Sizes

The solder droplet jetting method is much favorable for a small number of solder bumps and small bump size. In addition, the solder jetting method can fabricate various bump sizes without extra screen masks for screen printing or lithography masks for electroplating.

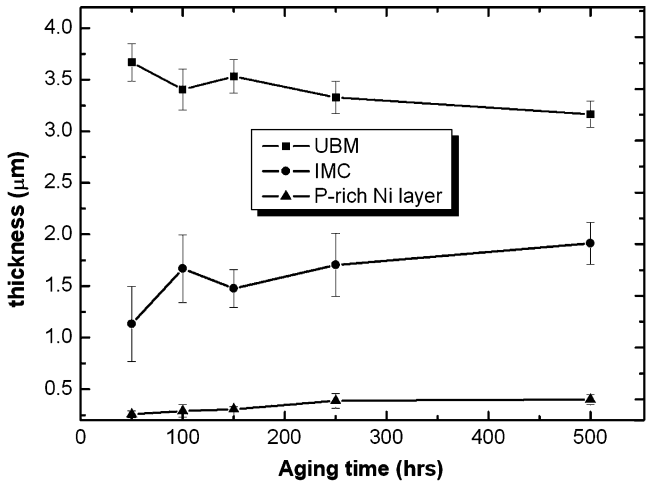

(a)

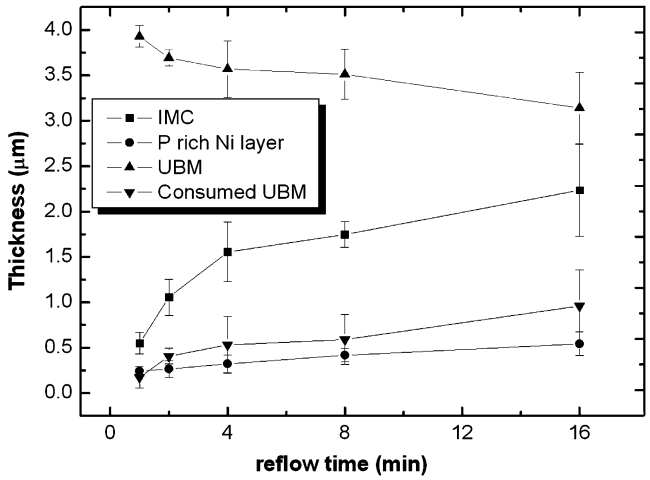

(b)

Fig. 12. Interfacial layers changes of Pb/63Sn solder bumps and electroless Ni–P/Au UBM (a) after solder reflow and (b) after aging.

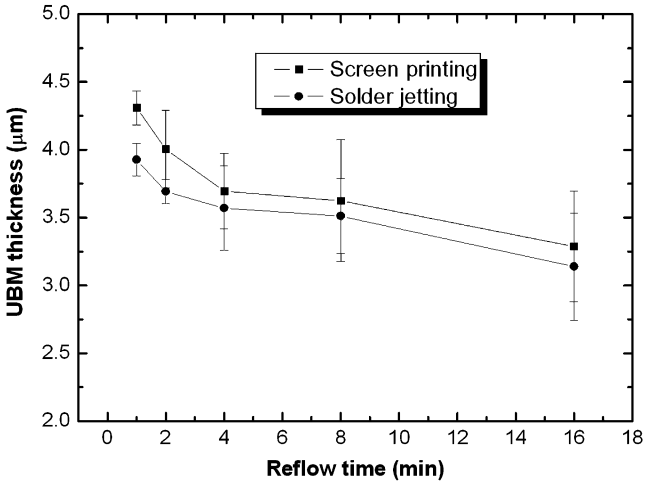

(a)

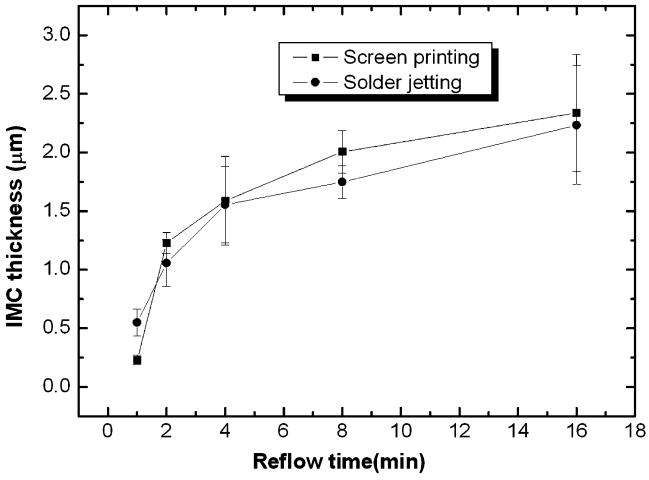

(b)

Fig. 13. Comparisons of interfacial reactions of Pb/63Sn solder bumps and electroless Ni UBM formed by solder droplet jetting and screen printing methods. (a) Electroless Ni UBM thickness changes. (b) IMC thickness changes.

The size of solder droplets just after jetting slightly increased as the fall time of the waveform induced to the jet nozzle increased. It was thought that the changes of droplet size presented in Fig. 15 resulted from the delay of solidification by the increase in fall time rather than the volume difference of solder droplets [7]. Similarly, it has been reported that the changes in form of the wave signal changed the droplet size for various ink jet materials in the drop-on-demand method [10].

To fabricate various size solder bumps, changing the number of droplets jetted on a pad was a better method than varying fall time. The multiple jetting made the lateral size and height of the solder bumps variable. In this case, in order to prevent a moving head touching the pile-up of droplets, a little delay between neighbor wave signals was used to lower the height of the pile-up by misaligning the center of the droplets. Using this method, reflowed solder bumps up to five solder droplets were formed on a 120-μm pad as shown in Fig. 16. A maximum of ten solder jetted droplets were successfully demonstrated in this study.

D. Applications on Real Devices

It is important to demonstrate the actual applicability of the solder droplet jetting method on real devices. To do this, Pb/63Sn solder bumps were formed on test chips with a DRAM pattern [Fig. 17(a) and (b)] and integrated passive devices [(c)] using the solder jetting method. Test chips with jetted solder bumps were flip-chip assembled on a printed circuit board, and then their bump-to-bump resistances were about 1.1–1.4 Ω. Low-pass filter integrated passive devices were jetted using Pb/63Sn solder jetting as shown in Fig. 18. The high-frequency characteristics of the solder jetted low-pass filter, measured by Yim, *et al.* [11], agreed well with those of low-pass filters fabricated by anisotropic conductive film (ACF) interconnection. The low-pass filters were designed so that a signal less than 900 and 1800 MHz could pass through them.

IV. Conclusion

In this research, jet conditions of stable solder droplets were optimized by the investigation of the effects of jet variables such as voltages and fall time of waveform parameters, jet height, overheating temperature, and substrate temperature. Using solder droplet printing, Pb/63Sn solder bumps were successfully fabricated on electroless Ni/Au UBM. As the

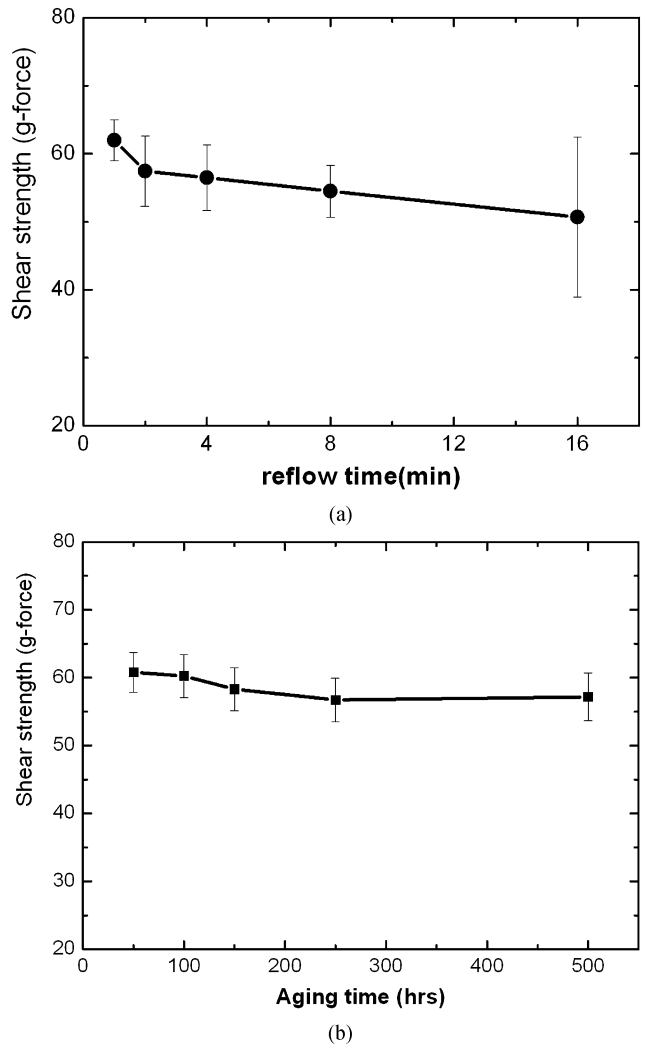

Fig. 14. Bump shear strength as a function of (a) reflow and (b) aging times.

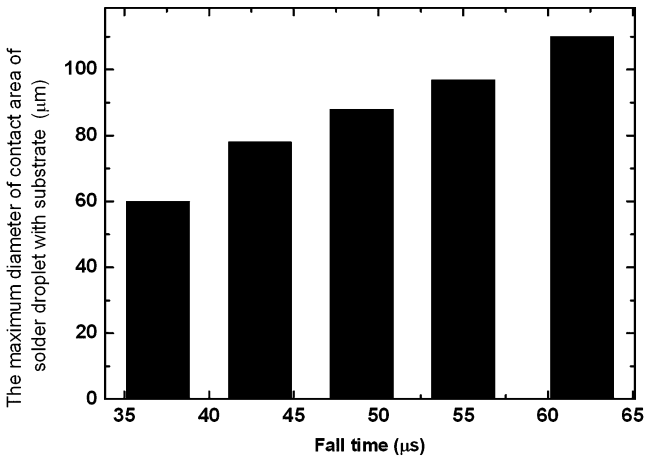

Fig. 15. Maximum diameter of solder droplets as a fall time of the wave signal.

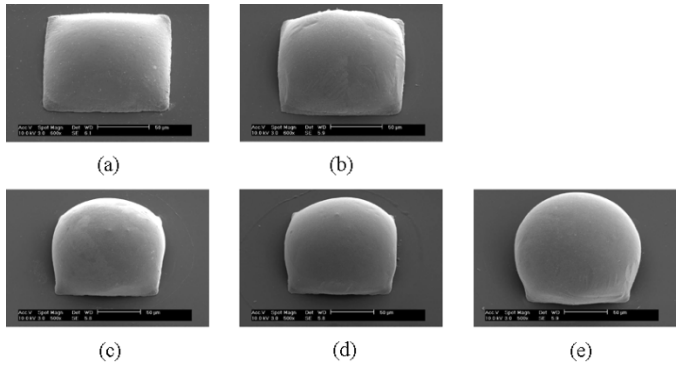

Fig. 16. Reflowed solder bumps with various heights by multiple droplets: 37-μs fall time and 120-μm pad size. (a) One droplet, 37.8 μm. (b) Two droplets, 55.8 μm. (c) Three droplets, 79.4 μm. (d) Four droplets, 97.5 μm, (e) Five droplets, 104.5 μm.

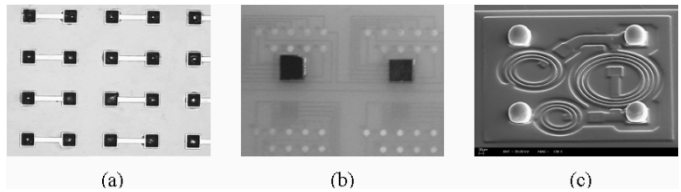

Fig. 17. Examples of real application. (a) Solder bumps after three droplets jetting on dog-born patterned wafer. (b) Test chips with DRAM pattern and PCB assembly. (c) Jetted solder bumps on 85-μm pad size of IPDs.

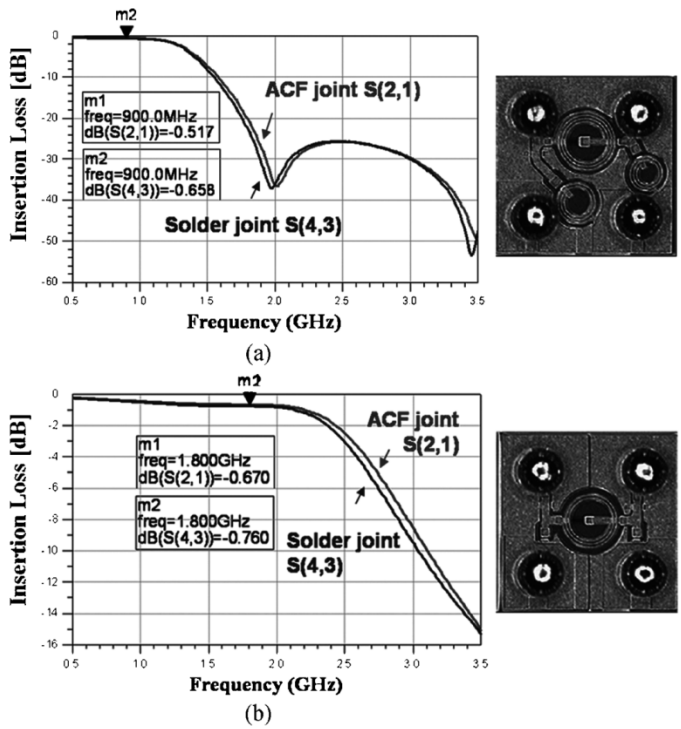

Fig. 18. High-frequency characteristics and images of jetted solder flip-chip by functional IC–RF IPD. (a) 900-MHz low-pass filter. (b) 1800-MHz low-pass filter [11].

second reflow time and aging time increased, Ni_3Sn_4 IMC grew and the consumption of electroless Ni UBM increased. The jetted Pb/63Sn solder bumps were successfully applied on conventional test chips with DRAM patterns and IPDs. Solder jetted IPDs were well operated as primarily designed in the high-frequency region. It was demonstrated that the solder droplet jetting method was an alternative bumping method that can form solder bumps with various sizes by increasing the number of solder droplets.

As mentioned in this paper, the solder droplet jetting method is the latest bumping technology with distinctive advantages,

such as smaller bump size, finer pitch, fewer process steps, and various bump sizes, in comparison with evaporation or screen-printing methods. It is also appropriate for a rework method of omitted solder bumps or in case that the number of solder bumps to be covered is relatively few. Moreover, high bumping speed, about 5–50 droplets per second, is one of the advantages of this method.

ACKNOWLEDGMENT

The authors would like to thank MicroFab Inc. for providing the technical equipment such as jet nozzles and jet head.

REFERENCES

[1] J. H. Lau, *Flip Chip Technologies*. New York: McGraw-Hill, 1996, pp. 123–126.
[2] W. R. Cox *et al.*, "Solder jet for low-cost wafer bumping," in *Proc. ISHM*, 1996, pp. 296–301.
[3] Q. Liu and M. Orme, "High precision solder droplet printing technology and the state-of-the-art," *J. Mater. Process. Technol.*, vol. 115, p. 272, 2001.
[4] E. Zakel, T. Teutsch, and R. Blankenhorn, "rocess makes electroless Nickel/Gold wafer bumping economical for flip-chip packaging," *Chip Scale Rev.*, pp. 67–71, Mar. 2003.
[5] D. J. Hayes, W. R. Cox, and M. E. Grove, "Micro-jet printing of polymers and solder for electronic manufacturing," *J. Electron. Manuf.*, vol. 8, no. 3 & 4, pp. 209–216, 1998.
[6] A. F. J. Baggerman and D. Schwazbach, "Solder-jetted eutectic PbSn bumps for flip-chip," *IEEE Trans. Compon., Packag., Manuf. Technol. B*, vol. 21, no. 4, pp. 371–381, Nov. 1998.
[7] J. M. Waldvogel and D. Poulikakos, "Solidification phenomena in picoliter size solder droplet deposition on a composite substrate," *Int. J. Heat Mass Transfer*, vol. 40, no. 2, pp. 295–309, 1997.
[8] Background on Ink-Jet Technology, MicroFab, Plano, TX, pp. 1–2, 1999. MicroFab Technote 99-01.
[9] "Drive Waveform Effects on Ink-Jet Device Performance," MicroFab, Plano, TX, 1999. MicroFab Technote 99-01.
[10] A. U. Chen and O. A. Basaran, "A new method for significantly reducing drop radius without reducing nozzle radius in drop-on-demand drop production," *Phys. Fluids*, vol. 14, no. 1, 2002. L2–L3.
[11] M. J. Yim *et al.*, "Flip chip interconnection using anisotropic conductive adhesives for RF and high frequency application," in *Proc. Electronic Components Technology Conf.*, 2003, pp. 1400–1402.

Ho-Young Son received the B.S. and M.S. degrees in materials science and engineering from the Korea Advanced Institute of Science and Technology (KAIST), Daejeon, Korea, in 2001 and 2003, respectively, where he is currently pursuing the Ph.D. degree in materials science and engineering.

His research interests are fine flip-chip interconnection using Cu column bumps and Pb-free solder bumping using a solder droplet jetting method.

Jae-Woong Nah (M'05) received the B.S. degree in metallurgical engineering from Korea University, Seoul, Korea, in 1997, the M.S. degree in metallurgical engineering from Seoul National University, Seoul, in 1999, and the Ph.D. degree in materials science and engineering from the Korea Advanced Institute of Science and Technology (KAIST), Daejeon, in 2004.

Following receipt of the Ph.D. degree, he joined the University of California, Los Angeles, as a Postdoctoral Research Associate. His research interests are flip-chip bumping process, electromigration in flip-chip solder joints, and reliability assessment of Cu/low-k interconnects.

Dr. Nah is a Member of IMAPS.

Kyung-Wook Paik (M'95) received the B.Sc. degree in metallurgical engineering from Seoul National University, Seoul, Korea, in 1979, the M.Sc. degree from the Korea Advanced Institute of Science and Technology (KAIST), Daejeon, Korea, in 1981, and the Ph.D. degree in materials science and engineering from Cornell University, Ithaca, NY, in 1989.

From 1982 to 1985, he was with KAIST as a Research Scientist and was responsible for various materials development such as gold bonding wire and nonferrous alloys. Following receipt of the Ph.D. degree, he was with General Electric Corporate Research and Development, Schenectady, NY, from 1989 to 1995, where he was involved with the R&D of materials and processes of GE High Density Interconnect (HDI) multichip module technology and power I/C packaging as a Member of the Senior Technical Staff. Since joining KAIST in 1995, he has been with the Department of Materials Science and Engineering as an Associate Professor, and he is currently working in the area of MCM, flip chip, MEMS, and display packaging. He had visited the Packaging Research Center at the Georgia Institute of Technology, Atlanta, as a Visiting Professor from March 1999 to February 2000, and was involved in the educational and integrated passives research programs. He has published more than 60 technical papers in the area of electronic packaging and currently holds 14 U.S. patents with four U.S. patents pending.

Dr. Paik is the Chairman of Korean IEEE-Components, Packaging, Manufacturing Technology chapter and is also a Member of IMAPS.